Journal of Geophysical Research: Atmospheres

RESEARCH ARTICLE
10.1029/2018JD028844

A TRMM Assessment of the Composition of the Generator Current That Supplies the Global Electric Circuit

Michael Peterson[1,2], **Wiebke Deierling**[3], **Chuntao Liu**[4], **Douglas Mach**[5], **and Christina Kalb**[1]

[1]National Center for Atmospheric Research, Boulder, CO, USA, [2]Earth System Science Interdisciplinary Center, Now at the University of Maryland, College Park, MD, USA, [3]Aerospace Engineering Sciences, University of Colorado, Boulder, CO, USA, [4]Texas A&M University Corpus Christi, Corpus Christi, TX, USA, [5]Global Hydrology and Climate Center, University of Alabama, Huntsville, AL, USA

Key Points:
- Electrified cloud satellite features are used to quantify individual current contributions to the Global Electric Circuit
- Thunderstorms contribute 61% of the total current, while electrified shower clouds provide the remaining 39%
- Tropical chimney Wilson current production is ranked: (1) the Americas, (2) Asia, and (3) Africa in contrast to Africa's lightning dominance

Correspondence to:
M. Peterson,
michaeljp24@gmail.com

Citation:
Peterson, M., Deierling, W., Liu, C., Mach, D., & Kalb, C. (2018). A TRMM assessment of the composition of the generator current that supplies the Global Electric Circuit. *Journal of Geophysical Research: Atmospheres*, *123*, 8208–8220. https://doi.org/10.1029/2018JD028844

Received 16 APR 2018
Accepted 12 JUL 2018
Accepted article online 24 JUL 2018
Published online 6 AUG 2018

Abstract The Peterson et al. (2015, https://doi.org/10.1175/JTECH-D-14-00119.1) passive microwave electric field retrieval is applied to 15 years of Tropical Rainfall Measuring Mission (TRMM) satellite observations to estimate the amount of Wilson current supplied to the Global Electric Circuit from individual electrified cloud features (ECFs), which are identified as contiguous precipitating cloud regions that produce Wilson current. Current contributions from 37 million ECFs sampled by TRMM are used to examine the composition of the DC generator current. Thunderstorms are found to supply 61% of the total retrieved current, while electrified shower clouds provide the remaining 39%. ECFs over land contribute 38% of the total current, while the ocean contributions are divided between coastal oceanic regions (35%) and the open ocean (27%). The greatest share of the total TRMM-retrieved current comes large mesoscale features ($>2 \times 10^3$ km^2 in area) and features that have peak 20-km electric fields in excess of 1 kVm^{-1}. This combination of extent and intensity leads to total currents greater than 10 A for a single ECF. The ranking of the tropical chimney regions by total current production is (1) the Americas (38%), (2) Asia (32%), and (3) Africa (15%). ECFs over the tropical Pacific Ocean contribute the remaining 15%. The Africa chimney is most prominent in total lightning activity but lags behind the others in total DC current due to a reduced frequency of electrified weather and weaker per-storm electric fields and Wilson currents compared to the other chimneys.

Plain Language Summary Tropical Rainfall Measuring Mission satellite observations are used to estimate the amount of current each tropical electrified cloud provides to the Global Electric Circuit. Collecting these estimates more than a decade makes it possible to quantify the importance of various cloud types and the distinct "chimney" regions for the global circuit. The majority of the global generator current is supplied by thunderstorms (61%), while electrified shower clouds that do not produce lightning provide the remaining current (39%). Most of this current comes from large mesoscale storms that have electric fields at 20-km altitude greater than 1 kVm−1 and individual current contributions exceeding 1 A. Of the three tropical chimney regions—the Americas, Africa, and Asia—Africa produced the most lightning, but the least current. This is because there are few electrified shower clouds in Africa compared to the Americas and Asia, and Africa thunderstorms appear to generate weaker electric fields and Wilson currents than their American and Asian counterparts.

1. Introduction

Charge imbalances in global electrified weather drive an atmospheric electrical circuit known as the Global Electric Circuit (GEC). C. T. R. Wilson's (1920) global circuit hypothesis described electrified clouds in terms of dipoles placed between the highly conductive ionosphere and surface of the Earth (Wilson, 1920). Because the lower atmosphere is not a perfect insulator, the positive and negative charges in the dipoles generate conduction current (Wilson current) in stormy regions that flows upward into the ionosphere. This generator current is counterbalanced by a downward-directed return current in fair-weather regions of the world. The GEC regulates the electrical potential of the ionosphere, which is generally around 240 kV relative to the surface of the Earth (Alderman & Williams, 1996; Markson, 2007).

In this GEC framework, changes to the generator current supplied by electrified weather correlate with the current densities and electric fields in the fair-weather load on the circuit. Much of the support for Wilson's global circuit hypothesis comes from comparing changes in the fair-weather electric field

measured at ground level with variations in global electrified weather. Early efforts focused on the response of the GEC to diurnal heating. Diurnal changes to the electric field over clean ocean regions on fair-weather days were measured during several nautical expeditions by the research vessels *Carnegie* and *Maud*. The universal time variation of the fair-weather electric field became known as the classic Carnegie curve (Israel, 1973: Appendix, Table XIX). The Carnegie curve was compared with the best available observations of global thunderstorm (TS) activity of the day by Brooks (1925), Whipple (1929), and Whipple and Scrase (1936). The diurnal cycles in TS activity were shown to be similar to the Carnegie curve, but with approximately twice the amplitude and notable differences in the shapes of the curves (Simpson, 1929; Williams & Heckman, 1993). Modern global lightning measurements confirm these discrepancies between the strength of the generator and the load on the circuit throughout the day (Bailey et al., 2007).

This mismatch implies that while land-based TSs are an essential source for the DC generator current, there are significant current contributions not represented in the lightning measurements. These missing current sources prevent a robust correlation with the climatological Carnegie curve and also the real-time fair-weather vertical current density (Holzworth et al., 2005). The most likely candidate for this missing current was initially thought to be contributions from electrified shower clouds (ESCs). ESCs have similar charge structures to their TS counterparts but do not initiate lightning. Thus, they would not be detected by lightning locating systems.

Electric field observations taken by National Aeronautics and Space Administration (NASA) aircraft passing over electrified weather (Blakeslee et al., 1999; Mach et al., 2009) have been used to quantify the conduction currents generated by individual TSs and ESCs in land and ocean regions (Mach et al., 2010). Measurements from 850 aircraft overflights revealed key differences in current output between land and ocean storms. Oceanic TSs produced, on average, 1.6 times the Wilson current of land-based TSs, while oceanic ESCs generated twice as much current as ESCs over land. In addition to demonstrating that electrified clouds without lightning do, indeed, contribute to the GEC, Mach et al. (2010) also suggest that separate scaling relationships between lightning flash rate and current output exist for land and ocean storms. These differences in land and ocean current output per storm are now considered to be the primary reason for the discrepancy between the classic Carnegie curve and the diurnal cycles of lightning and TSs.

Mach et al. (2011) used the aircraft overflight data from Mach et al. (2010) to adjust the diurnal cycle of lightning detected from space (Bailey et al., 2007) to account for ESC current contributions and differences in current output between land and ocean storms. This resulted in an agreement with the Carnegie curve to within 4% root-mean-square error except during two limited time periods. Subsequent analyses were performed using ground-based World Wide Lightning Location Network TS clusters, which also produced good agreements with the Carnegie curve (Hutchins et al., 2014; Mezuman et al., 2014).

Blakeslee et al. (2014) expanded on the Mach et al. (2011) results to compute seasonal variations in the diurnal cycles of total lightning measured from orbit and the corresponding total current supplied by electrified weather. These results were compared with modern ground-based fair-weather electric field measurements taken in Vostok Station, Antarctica, and found to be in good agreement throughout the year. The daily mean global total current is estimated to fluctuate from 2.4 kA in the northern hemisphere summer and 1.7 kA in the northern hemisphere winter.

The case of missing current contributions in the lightning-based approximations of the Carnegie curve touches on the larger issue of the composition of the global generator current. Since oceanic storms individually produce more current than storms over land (Mach et al., 2010), oceanic regions may rival the continents in terms of how much current they generate for the GEC. Liu et al. (2010) compare individual storm contributions using Tropical Rainfall Measuring Mission (TRMM) satellite precipitation feature (PF: Liu et al., 2008) rainfall products as a proxy for Wilson current. PFs enable the total current to be broken down according to feature metrics (i.e., storm type, region, and size) and the relative significance of different categories to be assessed.

Maps of rainfall from TSs and ESCs across the TRMM domain demonstrate that despite Africa's dominance in lightning, the Americas may be a more important source of current for the DC branch of the GEC. TSs supply 63% of the total current in this approach, while ESCs contribute the remaining 37%. Land-based electrified weather accounts for 42% of the total current compared to 58% for oceanic regions.

The key uncertainties with this approach lie in the static thresholds that divide ESCs from nonelectrified clouds and the use of total rainfall as a proxy for current output. The best agreement with the Carnegie curve in Liu et al. (2010) occurs when either ESC or oceanic contributions are ignored in contrast to Mach et al. (2011), which achieves a good fit with the Carnegie curve when both are considered. Blakeslee et al. (2014) provide similar seasonal analyses to Liu et al. (2010). Reasonable agreements are found with the fair-weather electric field in all seasons with oceanic and ESC contributions. The total current is divided between land-based TSs that supply 52% of the total, oceanic TSs that contribute 31%, and ESCs that supply the remaining 17% (15% from ocean storms and 2% from land storms).

The key strength of a feature-based approach such as Liu et al. (2010) is that it can elaborate on the relative importance of various storm types for the GEC. For example, the scale and precipitation structure of electrified clouds are important for current production. Mesoscale convective systems (MCSs) differ from ordinary TSs in their organization, longevity, and extent. They often include sizable stratiform regions that can become electrified through the advection of charged hydrometeors from the convective core and in situ generation (Ely et al., 2008; Lang & Rutledge, 2008; Rutledge & MacGorman, 1988). Model simulations indicate that while individual convective cells typically produce Wilson currents of around 0.4 A, the total current for mesoscale systems may be as high as 25 A (Davydenko et al., 2004). However, satellite observations indicate that MCSs account for only 1.2% of all storms globally (Nesbitt et al., 2000). The importance of MCSs relative to ordinary TSs is not clearly defined because while MCSs are 2 orders of magnitude less common, they have the potential to generate currents that are 2 orders of magnitude greater.

This study uses a TRMM PF implementation of the passive microwave electric field retrieval algorithm from Peterson et al. (2015) to estimate the current generated by individual electrified clouds. Retrieved currents are used to quantify contributions to the GEC based on geographical location, storm type, and according to feature properties that include lateral extent, the retrieved vertical component of the electric field at 20 km (E_z), and the total retrieved current. These contribution statistics compare the relative importance of electrified cloud types for the GEC according to the Peterson et al. (2015) retrieval.

2. Data and Methodology

The TRMM satellite was a unique platform for its comprehensive collection of meteorological instrumentation and 17 years spent in low-Earth orbit. Coincident measurements taken by its precipitation radar (PR), passive microwave imager (TRMM Microwave Imager: TMI), Visible and Infrared Scanner, and optical lightning detector (Lightning Imaging Sensor: LIS) are available throughout the tropics up to 36° latitude (Kummerow et al., 1998) between 1997 and 2015.

The passive microwave algorithm from Peterson et al. (2015) is applied to 15 years of collocated PR and TMI orbital swaths to quantify the electric fields above electrified clouds at a constant 20-km altitude. Passive microwave measurements at 85 GHz reflect column ice water content that is important for noninductive charging (Jayaratne et al., 1983; Mansell et al., 2005; Reynolds et al., 1957; Saunders & Peck, 1998; Saunders et al., 1991; Takahashi, 1978; Takahashi & Miyawaki, 2002). The algorithm uses the 85-GHz brightness temperature swath to create a simplified physical model of the spatial distribution of charge in each observed electrified cloud. It then applies Coulomb law to this model to approximate the electric field that would be measured at a given location over the storm.

The passive microwave proxy is converted into an electric field estimate using frequency- and resolution-dependent empirical transfer functions constructed from coincident electric field and passive microwave measurements taken by the NASA ER-2 aircraft (Mach et al., 2009). For every second of data over the course of hundreds of overflights, the electric field measured at the aircraft location (nominally 20-km altitude) is compared to the passive microwave scene below. Hundreds of thousands of points of comparison fill in the relationship between the raw passive microwave proxy that is output by the algorithm and the measured electric field. Calculations are repeated for every grid point in the passive microwave swath to retrieve the electric field at all points above each electrified cloud observed by TRMM.

The TRMM implementation of this algorithm differs from the ER-2 implementation in the following key areas. The availability of polarization-corrected temperatures (Spencer et al., 1989) throughout the TRMM record removes the ocean artifact issue that was prevalent with the ER-2 data (Peterson et al., 2015). However,

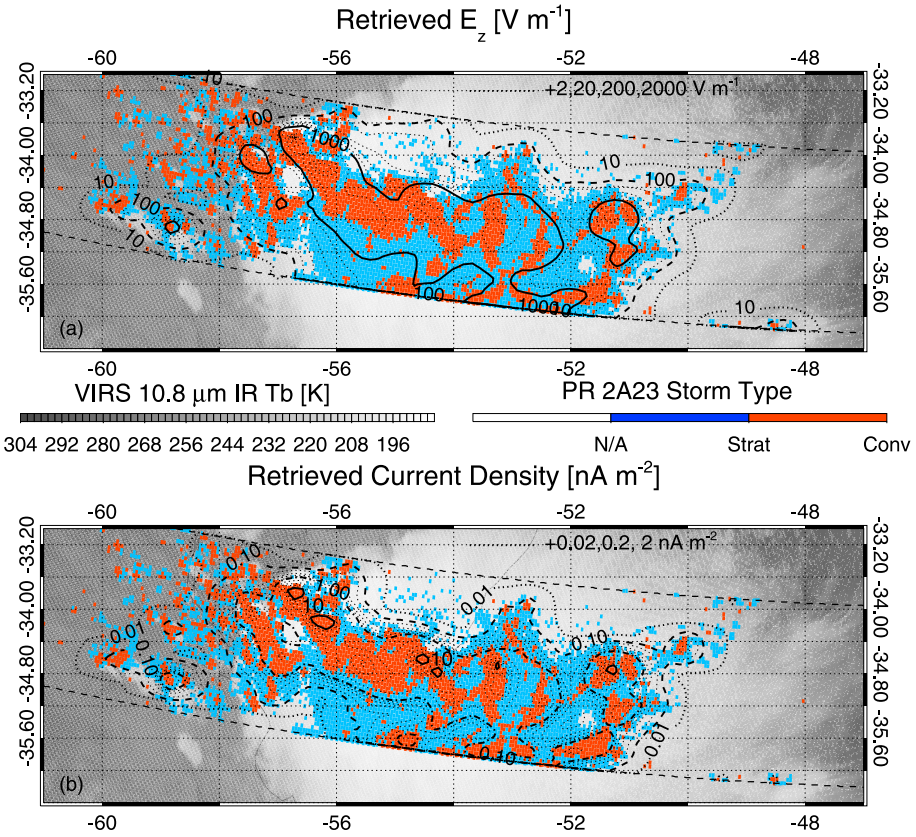

Figure 1. The retrieved vertical component of the (a) electric field and (b) current density for an example mesoscale convective system case. PR 2A23 rain types (color) are overlaid on Visible and Infrared Scanner infrared brightness temperatures (gray). Electric fields and current densities are plotted as isocontours.

while this source of terrain-based artifacts is not present with TRMM, snow cover in high-altitude regions adds a new source of artifacts for the satellite implementation. Thus, TMI pixels over mountainous regions where the elevation exceeds 3 km are not considered. Additionally, TMI pixels that occur outside of the comparably narrow PR swath are omitted. Previous versions of the algorithm used a passive microwave lookup table to constrain the vertical extent of the electrified cloud. However, the availability of 3-D PR reflectivity data makes it possible to accurately prescribe the height of the electrified cloud within this common swath. Electrified clouds are not allowed to exceed a height of 19 km, however, as a distance square term in the calculations leads to unphysical electric field estimates when the 20-km observer is too near the electrified cloud.

An example TRMM overpass of an MCS case is shown in Figure 1. Infrared brightness temperatures (grayscale) depict the horizontal extent of the feature compared to the PR swath (dashed thin lines). The precipitation type along the swath is identified by the TRMM 2A23 algorithm (Awaka et al., 1998) as either convective (red) or stratiform (blue) where rainfall is detected. Isocontours of retrieved E_z are overlaid in Figure 1a. Major contours (factors of 10) are shown as thick contour lines (dotted: 10 Vm^{-1}, dashed: 100 Vm^{-1}, solid: 1 kV^{-1}), while thin dotted contours are drawn for every 2, 20, 200, or 2000 Vm^{-1} in between. The strongest electric fields in this intense storm are found in the convective core with typical values exceeding 1 kVm^{-1} and peak values as high as 8 kVm^{-1}. For comparison, peak E_z values measured by the ER-2 aircraft in Mach et al. (2009) range from 1.1 to 8.8 kVm^{-1} (overflights from 1993 to 2005 only).

Current densities are computed by multiplying the retrieved electric fields by a typical atmospheric conductivity at 20-km altitude. ER-2 conductivity measurements in the tropics range from 1.8 to 3.0 pSm^{-1} in Mach et al. (2009). As we are concerned with differences in current contributions from microphysical variations in convective clouds rather than conductivity changes, we apply a representative value of 2.4 pSm^{-1} to all

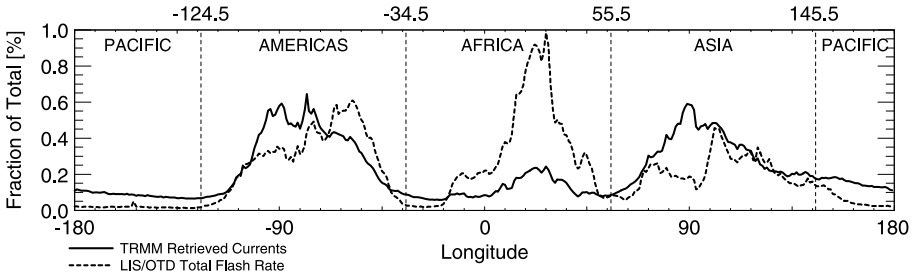

Figure 2. Distribution of total retrieved current (solid) and Lightning Imaging Sensor/Optical Transient Detector lightning activity (dashed) by longitude.

TRMM orbits. Analysis of coupled variations in convection and atmospheric conductivity are planned for future work using numerical conductivity models (e.g., Baumgaertner et al., 2013). The retrieved current density for the case in Figure 1a is shown in Figure 1b. The peak current densities for the maxima (closed contours) in convective regions range from 10 and 20 nA m^{-2} in each case. The strongest current densities in the 850 overflights from Mach et al. (2009) were between 31 and 38 nA m^{-2}.

The total storm current is computed by integrating the retrieved current density across the electrified cloud region of interest. We cluster the pixel-level orbital data into radar PFs (RPF; Liu et al., 2008) based on contiguous regions of near-surface rainfall. Total RPF currents are estimated by integrating the current densities produced by convection across the feature footprint. The algorithm can produce reasonable estimates of stratiform electric fields, but the stratiform currents are not considered reliable (Peterson et al., 2017, 2018). This is largely due to a lack of polarity information in the algorithm. ER-2 (Deierling et al., 2014) and balloon (Marshall et al., 2009) electric field measurements, as well as lightning observations (Lang et al., 2004; Williams, 1998), associate electrified stratiform clouds with inverted-polarity storms and atmospheric electrical processes. The algorithm essentially assumes that all electrified clouds consist of positive dipoles in accordance with Wilson's (1920) global circuit hypothesis. Thus, inverted dipoles that would discharge the GEC instead add current to the circuit in the retrieval. The result is a stratiform current contribution that even exceeds convection in cases like the example in Figure 1. Thus, we focus on convection, assuming that the global average net current contribution from stratiform clouds is negligible.

Electrified cloud features (ECFs) are defined as RPFs that the retrieval identifies as producing conduction current. Unlike most feature-level studies (i.e., Liu et al., 2010), we do not enforce a minimum size requirement on the features we consider. An ECF may be composed of a single pixel or hundreds of pixels. ECFs are classified as TSs if LIS detects a lightning flash centered within the feature boundary. The remaining ECFs are considered ESCs. As in Liu et al. (2010), low flash rate TSs may be identified as ESCs if no lightning is detected in the $<$~90-s window when LIS is above the storm.

Collocated PR and TMI observations are used to characterize the size, intensity, and precipitation structure of each ECF. The peak electric field and total current are also recorded. These properties are integrated into an ECF database of 37 million features that will be used to quantify contributions to the total generator current. It is important to emphasize that these current contributions are subject to the limitations of the retrieval and may change as the algorithm improves. The lack of polarity information and inability to correctly represent stratiform currents constitute a serious unknown in this methodology. Likewise, the relatively coarse pixel size of TMI (5×7 km at 85 GHz at launch) limits the ability of the current algorithm to characterize small convective cells that may be important for the GEC. If the TMI grid is not perfectly aligned with a TS that is just a few pixels in size, then clear air regions (at ~300 K) will contaminate the 85-GHz brightness temperature measurements of the electrified cloud. These factors should be kept in mind when assessing the reported relative current contributions.

3. Results

The total generator current within the TRMM domain is totaled by longitude and compared with the LIS/OTD lightning flash rate climatology from Cecil et al. (2014) in Figure 2. Both distributions have three distinct peaks

Table 1
Electrified Cloud Feature (ECF) Counts and Total Current Contributions From Thunderstorms and Electrified Shower Clouds (ESCs) in Land, Coastal Ocean, and Open Ocean Regions

	All ECFs		Thunderstorms		ESCs	
	Count	Current	Count	Current	Count	Current
TRMM domain	**100%**	**100%**	**1%**	**61%**	**99%**	**39%**
Land	**8%**	**38%**	0.73%	33%	7.5%	5.2%
Coastal ocean	**27%**	**35%**	0.32%	21%	26%	14%
Open ocean	**65%**	**27%**	0.11%	7.3%	65%	20%

Note. Totals for each region and storm type are bolded.

over the continental land masses. Currents are reduced between continents, while lightning is hardly apparent over the Atlantic and Pacific basins. The three peaks are known as the tropical continental chimneys of the Americas, Africa, and Asia (Williams & Satori, 2004). We leverage the fact that these peaks are separated by approximately 90° longitude to define equal-area longitude quadrants surrounding the continental chimneys (dashed lines in Figure 2).

The distributions of lightning and storm current differ not only by land and ocean, as noted previously, but also by chimney. Africa is dominant in terms of lightning followed by the Americas, and then Asia. The Africa chimney contributes significantly less DC current than the other chimneys, however. In the following sections, we will examine the current contributions from electrified clouds that result in the totals for land and ocean regions (section 3.1) and for the tropical chimneys (section 3.2).

3.1. Current Contributions in Land and Ocean Regions

The contributions to the global generator current from TSs and ESCs in land and ocean regions are quantified in Table 1. Land is distinguished from ocean at the shoreline, while the ocean is divided into two subregions: coastal ocean within 1,000 km of shore and the open ocean beyond. The continents contain 8% of all electrified clouds observed by TRMM but contribute 38% of the total current. The remaining 62% of the total current is divided between the 27% of ECFs over the coastal ocean (35% of the total current) and the 65% of ECFs over the open ocean (27% of the total current). TSs account for 1.2% of all ECFs and contribute 61% of the total current. ESCs contribute 39%, with most this current coming from open ocean ESCs.

Fractional current contributions from TSs and ESCs are reported in Mach et al. (2011). Using the aircraft overflight current data to estimate the total current from the satellite lightning climatology yields a 55% (32%) contribution from land (ocean) TSs and 2% (11%) contribution from land (ocean) ESCs. However, these results are subject to an aircraft sampling bias that prioritizes TSs over ESCs as most storm types of interest for a given field program produce lightning. Mach et al. (2011) account for this by artificially increasing the number of ESCs and recomputing the current totals.

The best match to the Carnegie curve is found when it is assumed that the NASA aircraft underestimate the number of ESCs by a factor of 4. The current contributions in this case become 40% (23%) from land (ocean) TSs and 6% (31%) from land (ocean) ESCs. These results from Mach et al. (2011) also best match our 60%–40% split between TS and ESC contributions and 40%–60% split between land and ocean contributions.

The agreement between our retrieved total current contributions and the Mach et al. (2011) currents is notable because we make no supposition about differences in current output from land and ocean storms or from TSs and shower clouds. The retrieved currents depend only on the observed passive microwave and radar measurements of the clouds. Terrain classification and storm type (ESC or TS) are assigned after the electric field calculations while creating PFs. We can thus account for the land and ocean differences in overall current production in Mach et al. (2011) with the measured variations in microphysical properties of electrified weather in these regions.

We further compute the average currents and peak electric fields ($E_{z\text{-max}}$) for land and ocean TSs and ESCs in Table 2 for comparison with the aircraft results presented in Mach et al. (2010). Land-based TSs account for

Table 2
Electrified Cloud Feature Counts as a Fraction of the Global Total Number of Thunderstorms (TSs) or Electrified Shower Clouds (ESCs) and the Mean Properties for Land and Ocean TSs and ESCs

	All		Land		Coastal ocean		Open ocean	
	TS	ESC	TS	ESC	TS	ESC	TS	ESC
Frequency [%]	100	100	55	6	31	27	14	67
Mean $E_{z\text{-max}}$ [Vm^{-1}]	888	37.3	902	128	928	40.1	749	22.1
Mean current [A]	1.28	0.049	0.99	0.066	1.64	0.056	1.81	0.046

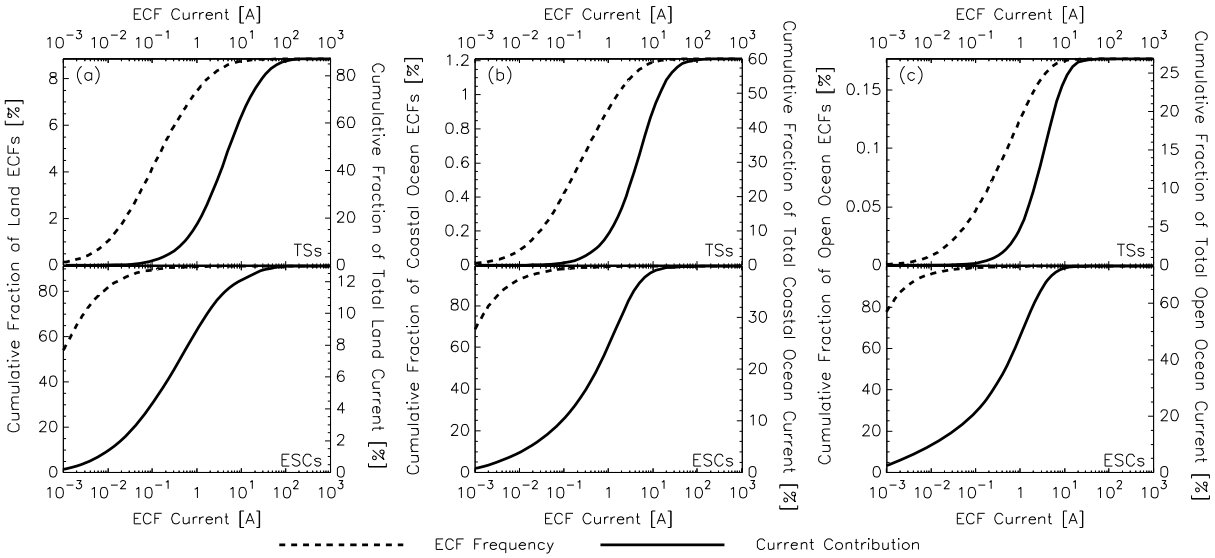

Figure 3. Cumulative number (dashed) and current (solid) contributions from (top row) thunderstorms and (bottom row) electrified shower clouds by individual electrified cloud feature Wilson current in (a) land, (b) coastal ocean, and (c) open ocean regions.

55% of ECFs with lightning. On average, the strongest electric fields in these ECFs are 902 Vm^{-1} and the total feature current is 0.99 A. ECF TSs over the coastal ocean, meanwhile, account for 31% of all TSs and produce average peak electric fields of 928 Vm^{-1}. The average total current in these storms is 1.64 A. The remaining 14% of TSs occur over the open ocean with peak electric fields of 749 Vm^{-1} and total currents of 1.81 A, on average. The average TS currents in Mach et al. (2010) were 1.0 A over land and 1.6 A over the (coastal) ocean. Thus, the mean ECF TS total currents produced by the passive microwave retrieval agree with Mach et al. (2010), further supporting the idea of a microphysical origin for their land and ocean differences.

The ESC currents produced by the passive microwave retrieval do not agree with the average values in Mach et al. (2010), however. While ESCs, on average, generate 0.13 A over land and 0.39 A over the ocean in Mach et al. (2010), the average ESC total currents in our ECF database are 0.065 A for land, 0.056 A for the coastal ocean, and 0.045 A for the open ocean. The average current per ECF shower cloud is on the order of one half (land) or one seventh (ocean) of the aircraft values because of aircraft sampling biases (discussed in Mach et al., 2011) and because the ECF database includes a substantial number of weak features that contain only a few pixels producing any current. The average peak electric field in these ESCs is only 37 Vm^{-1} overall and varies between 22 Vm^{-1} over the open ocean and 128 Vm^{-1} over land. Most of these small features would be removed if we enforced a minimum size threshold as in Liu et al. (2010).

We can quantify the importance of these ubiquitous weak ESCs for the global generator current by summing their contributions and comparing with the overall total. Distributions of the total current supplied by ECFs according to their individual retrieved Wilson current are shown in Figure 3. TS contributions (top row) and ESC contributions (bottom row), together, add up to 100% for land (Figure 3a), coastal ocean (Figure 3b), and open ocean (Figure 3c) regions. Cumulative ECF counts (dashed lines) are shown on the left axis of each plot, while cumulative current contributions (solid lines) are shown on the right axis. As in Table 1, the TS ECF count over land (Figure 3a) peaks at 8% of the overall total, while the TS current contribution peaks at 86% (i.e., 33% of the global current for land TSs per 38% of the global current for all land ECFs).

The largest contribution to the TS total current comes from ECFs that individually produce between 1 and 25 A. Though 30% of TS ECFs produce 50 mA or less, their contribution is negligible compared to these stronger storms. Similarly, 55% (land) to 77% (open ocean) of ECFs produce <1 mA of current and have only a marginal contribution to the total. ESCs contribute significantly to the total current over a larger range of individual Wilson currents than TSs. Most ESCs in the ECF database produce <1 mA of current, but these storms contribute $<1\%$ of the total land and coastal ocean currents, and $<3\%$ of the total open ocean current. The average ESC from Table 2 produces ~50 mA. Over land, ESCs that generate 50 mA or less

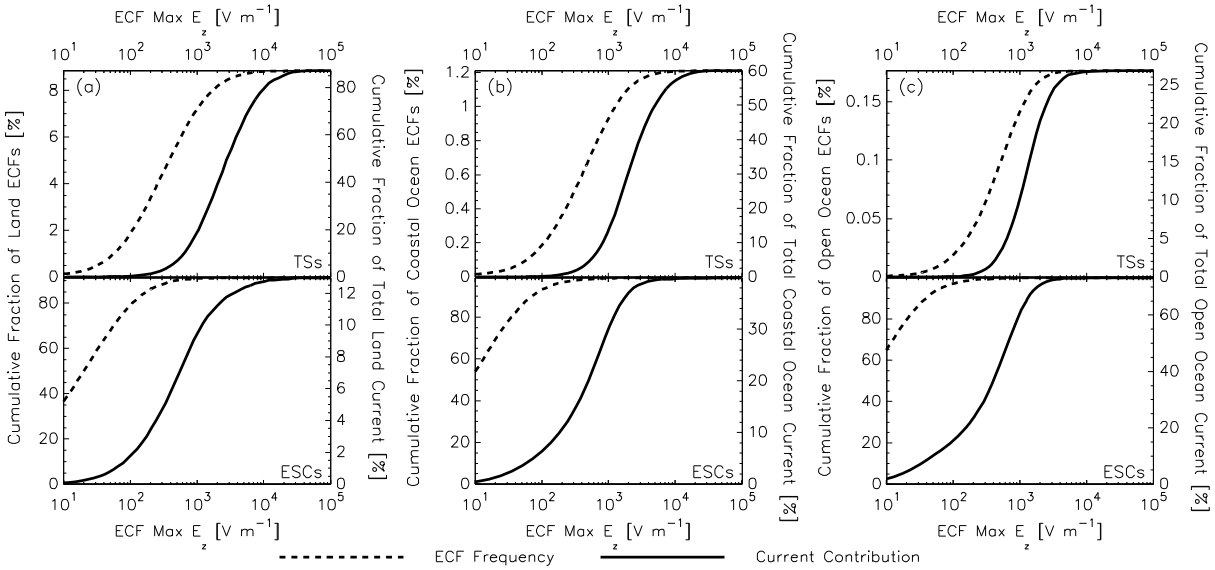

Figure 4. The same as Figure 3 for cumulative number and current contributions by electrified cloud feature peak vertical electric field.

contribute 3.3% of the overall current and 25% of the total ESC current. ESCs that produce <50 mA over the coastal ocean contribute 8% of the overall current and 21% of the ESC current, and over the open ocean contribute 17% of the overall current and 23% of the ESC current. ESCs that generate more than 0.13 A over land or 0.39 A over the ocean (average values from Mach et al., 2010) supply the majority of the total ESC current (60% for land and 52% for the coastal and open ocean).

Electrified cloud features that individually contribute more than 25 A can be noted in the current distributions in Figure 3. Only 30 ECFs in every million (or four TSs in every thousand) generate a Wilson current exceeding 25 A, but their combined contribution accounts for 8% of the total generator current. The example case in Figure 1 is one such storm with a total Wilson current of 70 A. An ECF may achieve a Wilson current greater than any case surveyed by the NASA aircraft by either having particularly high electric fields (and current densities) or by covering a much larger contiguous area than the storm regions sampled in a typical overflight.

Cumulative ECF contributions by peak electric field strength are shown in Figure 4. Almost the entire TS current contribution comes from storms with peak E_z values between 100 Vm^{-1} and 10 kVm^{-1}, while ESCs with peak E_z values as low as 10 Vm^{-1} provide significant contributions to the ESC total. The strongest retrieved E_z values in the ECF database are between 30 and 40 kVm^{-1}. This equates to a current density between 72 and 96 nA m^{-2}. The strongest measured electric fields in Mach et al. (2009) are 8.8 kVm^{-1} for the ER-2 and 15.9 kVm^{-1} for the Altus aircraft, and the highest current densities are between 30 and 40 nA m^{-2}.

Such extreme peak electric fields could suggest that placing a maximum charge height threshold at 19 km is not sufficient for removing artifacts from exceptionally tall storms. It is also possible that these retrieved values are physical and result from cases of extreme convection that would not be measured by aircraft. TRMM has had 17 years to sample the strongest weather on Earth (Zipser et al., 2006) with no aversion to passing directly over the most intense storms. Even though the highest retrieved electric fields exceed the strongest observations by NASA aircraft in Mach et al. (2009), they only differ by approximately a factor of two. Regardless, the absolute strongest storms have little impact on the overall current, while two third of the high current ECFs—including the example in Figure 1—have peak E_z values within the range measured by aircraft in Mach et al. (2009). Anomalously high current densities, alone, do not account for individual ECFs having total currents in excess of 25 A.

The ECF size spectrum provides an alternate explanation for features with exceptional total currents. ECFs are not always individual dipoles as envisioned by Wilson, but rather amalgamations of many convective cells connected by a common raining area. The MCS in Figure 1 clusters more than 40 separate convective features spread across a 730-km swath into a single ECF. The average current contributed by each of these

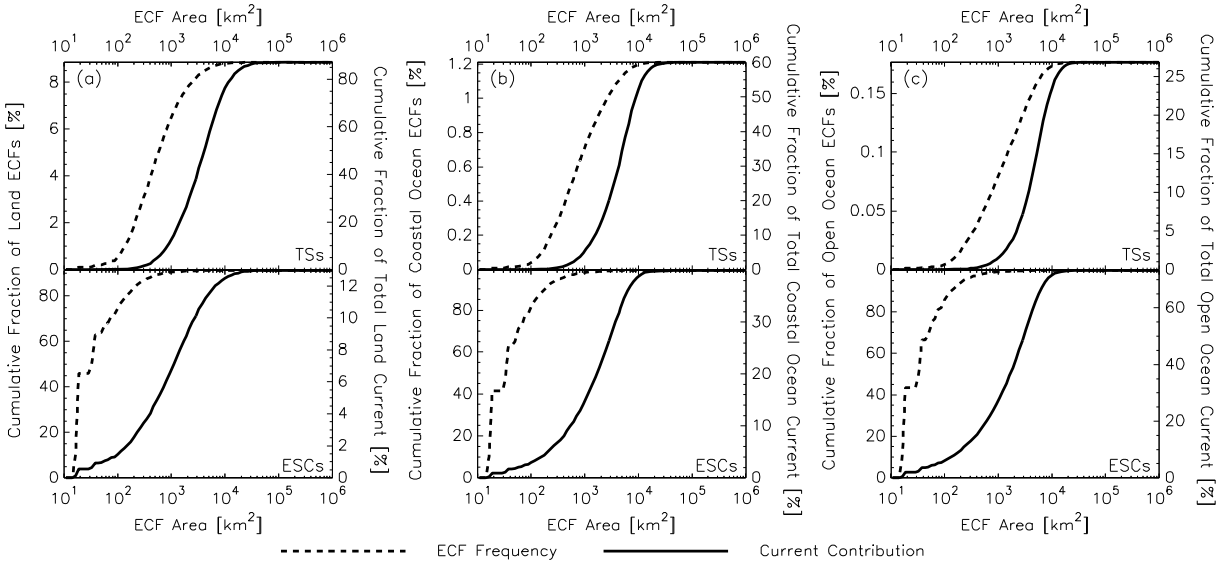

Figure 5. The same as Figure 3 for cumulative number and current contributions by electrified cloud feature area.

features is roughly 1.75 A. Rather than showing the size differences in individual convective dipoles, the ECF size spectrum differentiates between cases of isolated convective cells on the low end and organized convective systems on the high end.

Distributions for the cumulative frequency and current contribution by ECF area are shown in Figure 5. The small ECFs ($<$75 km^2) that were excluded in Liu et al. (2010) increase the sample size by ~200%. If we define the convective scale as having a scale length $<$ 10 km, then 87% of ECFs would be convective-scale storms. Almost all of these features (99.90%) are ESCs with average peak electric fields around 15 Vm^{-1} at 20-km altitude and total currents $<$1 mA. The total current produced by all convective-scale ECFs accounts for just 3% of the overall total. The remaining 13% of ECFs extend into the mesoscale and supply 97% of the total current. For comparison purposes, we distinguish MCSs that have characteristic dimensions of 100 km in length and 20 km in width for an overall area of 2,000 km^2. This is the same area threshold used to identify large features in Liu et al. (2008). These MCSs account for the top 0.36% of ECFs in terms of feature area but contribute 64% of the total current. Large MCSs have an average Wilson current of 2.8 A per feature. Thus, while convective-scale features are 270 times more frequent than MCSs, MCSs produce 5,000 times more current than the average convective-scale feature.

Mesoscale features are particularly important in terms of TS contributions (top row in Figure 5). Most TS contributions come from storms that range in size from 10^3 to 10^4 km^2 compared to 10^2 and 10^4 km^2 for ESCs. Mesoscale contributions from oceanic ECFs are also slightly increased compared to their land-based counterparts. The extreme sizes of these ECFs explain why they can individually contribute high total currents. The smallest ECF that produces $>$25 A is 2,200 km^2 in area, and the largest is 46,000 km^2. The retrieved electric fields and current densities are not unreasonable compared to the ER-2 measurements (i.e., Figure 1). Instead, it is the horizontal scale of these electrified clouds that is exceptional and allows them to play a significant role in the GEC.

3.2. Current Contributions in the Tropical Chimney Regions

Electrified cloud feature properties and current contributions can also be used to provide insights into the ranking of the tropical chimney regions for the DC circuit. TRMM observations are used to repeat the diurnal comparison from Whipple (1929) between electrified cloud area from each of the chimneys (thunder area in the original work) to the total DC current (the Carnegie curve, originally) in Figure 6. The total electrified cloud area curve peaks at 18:00 UTC and reaches a minimum at 2:00 UTC. ESCs over the Pacific quadrant are the largest contributor to ECF area for all times. The Americas and Asia contribute similar quantities of electrified cloud area to the total, and Africa universally contributes the least.

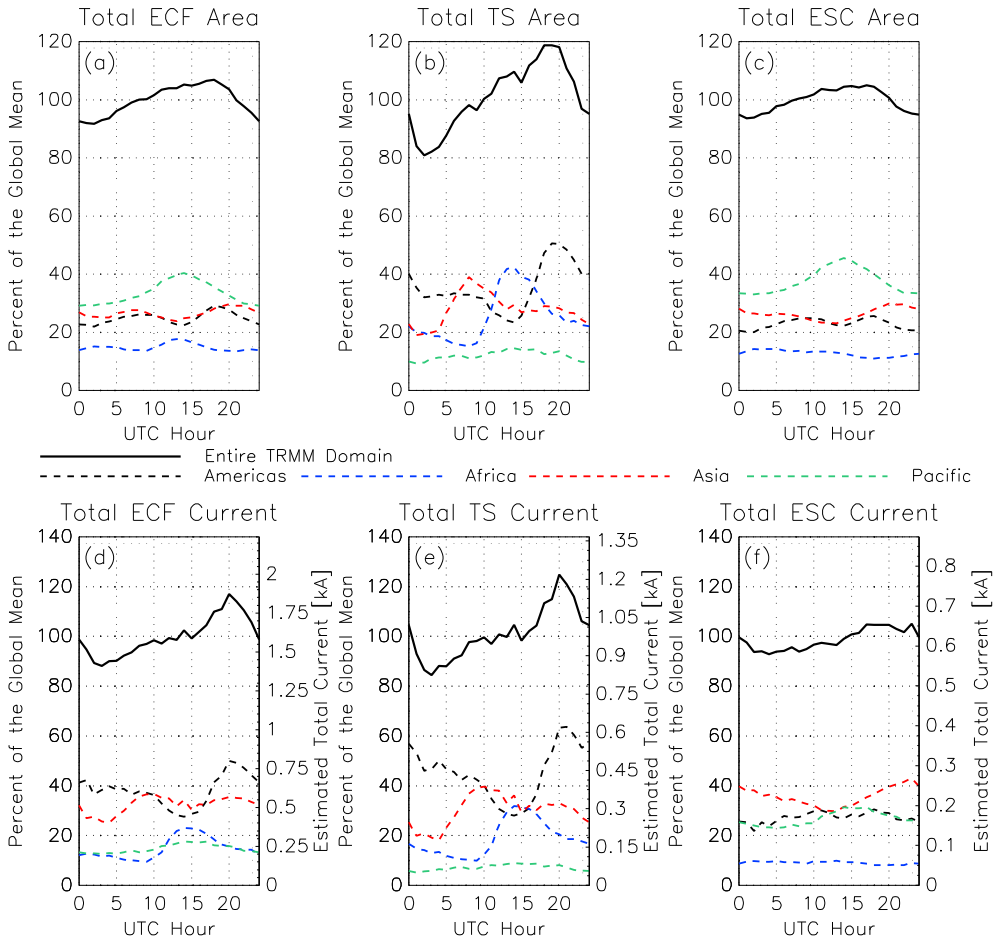

Figure 6. The diurnal cycle of (top row) electrified cloud area and (bottom row) total electrified cloud feature (ECF) current for all (a and d) ECFs, (b and e) thunderstorms, and (c and f) ESCs. Individual contributions from the Americas (dashed, black), Africa (dashed, blue), Asia (dashed, red), and the Pacific (dashed, green) are shown in addition to the global total (solid, black).

The chimney contributions to electrified cloud area depend largely on the frequency of TSs and shower clouds in each region. The TS area curves for the individual chimneys (Figure 6b) have distinct peaks at 8:00 UTC for Asia, 14:00 UTC for Africa, and 20:00 UTC for the Americas, as in Whipple (1929). The TS area curve for the Pacific quadrant is largely flat by comparison with a peak at 15:00 UTC. The Africa chimney is reduced compared to Whipple's analysis, however. Rather than being the dominant chimney in terms of TS area, it comes in second between the Americas and Asia. Because of this, the TRMM TS area curve more closely resembles the shape of the classic Carnegie curve than the early 20th century comparisons (Whipple & Scrase, 1936).

The diurnal cycles of ESC area for each of the chimneys are shown in Figure 6c. The ESC area curves are largely flat for the tropical chimneys and partially support the early view of oceanic TSs and ESCs adding essentially a constant background current to the diurnal cycles of TSs in the land-based chimneys (Whipple, 1929). The key departure from this view is the Pacific quadrant, which is responsible for the largest fraction of total ESC area. The Africa chimney contributes least to the total electrified cloud area due to its lack of ESC area. The TS area from Africa is competitive compared to the other chimneys, but the ESC area is only half of either the Americas or Asia.

The separation of the land masses can also be noted in the electrified cloud area curves in Figures 6a–6c. Since the four quadrants are separated by one fourth of the globe, we expect a 6-hr phase difference between adjacent quadrants. Indeed, the peaks of the Americas and Asia curves and the Africa and Pacific

Table 3
Electrified Cloud Feature Counts as a Fraction of the Global Total Number of Thunderstorms (TSs) or Electrified Shower Clouds (ESCs) and the Mean Properties for TSs and ESCs in Each Longitude Quadrant

	Americas		Africa		Asia		Pacific	
	TS	ESC	TS	ESC	TS	ESC	TS	ESC
Frequency [%]	34	23	30	14	27	24	7.8	39
Mean area [km^2]	1,459	87	1,205	82	1,452	95	2,222	84
Mean $E_{z\text{-max}}$ [Vm^{-1}]	970	37	713	21	922	38	670	70
Mean current [A]	1.5	0.04	0.72	0.02	1.2	0.03	1.1	0.008

curves on opposite sides of the globe largely agree in phase in Figure 6a. Two peaks can be noted in the Americas and Asia curves. These correspond to maxima in land-based and oceanic convection that are both frequent in these regions (Hendon & Woodberry, 1993; Liu & Zipser, 2008; Nesbitt & Zipser, 2003; Peterson & Liu, 2011). Land-based total electrified cloud area peaks in the local afternoon, while oceanic total electrified cloud area peaks in the local early morning hours. The 7:00–9:00 UTC peak corresponds to the land-based maximum in Asia electrified cloud area, and the oceanic maximum in Americas electrified cloud area. The reverse is true for the 18:00–20:00 UTC peak. The Africa and Pacific quadrant curves have a single peak at 14:00 UTC because electrified weather in these regions is dominated by a single terrain type: land for Africa and ocean for the Pacific.

Chimney contributions to the diurnal cycle of total ECF current are shown in Figures 6d–6f. Values are reported as fractions of the global mean, and in Amperes extrapolated to the poles using the approximation from Peterson et al. (2017). The Americas and Asia contribute the most current with a slight edge for the Americas due to a larger TS contribution (Figures 6b and 6e). Africa and the Pacific both contribute about half as much current as other quadrants. The Pacific quadrant lags behind the Americas and Asia chimneys because, while it has an enormous amount of ESC area (Figure 6c), it lacks the TS area to compete with the chimney regions (Figure 6b). Africa, however, has a slight edge in TS area over Asia but still falls short in total current. This is due to there being very little ESC area in Africa compared to the other chimneys and because African TSs produce less total current than their American and Asian peers (Figure 6e).

Africa stands out on the individual ECF level as well as in these global total statistics. The fractions of ECFs in each quadrant and their average properties are listed in Table 3. TS counts are divided relatively evenly between the chimneys with 34% located in the Americas 30% in Africa and 27% in Asia. The remaining 8% are located in the Pacific quadrant. Africa has only 60% the number of shower clouds as the other chimneys, consistent with the TS and ESC area curves in Figures 6b and 6c. The average African TS is 200 km^2 smaller compared to its Americas or Asia counterpart, however. The average peak electric field is also reduced at 713 Vm^{-1} compared to 970 Vm^{-1} for the Americas and 922 Vm^{-1} for Asia. This combination of a slightly reduced area and notably weaker electric fields leads to the average African TS generating around half the total current as its peers in adjacent chimneys. Current production from individual African TSs is even smaller than TSs in the Pacific quadrant, which have the lowest $E_{z\text{-max}}$ values (670 Vm^{-1}) but the largest areas (2,222 km^2).

African TSs may be particularly efficient at generating lightning, but their microphysical properties suggest that they are not well-suited for generating strong DC Wilson currents. The ranking of the longitude quadrants in terms of total generator current is (1) the Americas, (2) Asia, (3) the Pacific, and (4) Africa. The muted peak over Africa in Figure 2 prevents the 15:00 UTC peak that can be seen in the diurnal cycles of lightning (i.e., Figure 1 in Bailey et al., 2007) from forming in our analyses. This allows our total retrieved currents in Peterson et al. (2017) to more closely match the Carnegie curve.

4. Conclusion

Tropical Rainfall Measuring Mission retrievals of the Wilson current supplied by individual electrified clouds are used to examine the composition of the global DC generator current for the GEC. Current contributions from land and ocean regions, TSs and ESCs, and based on the individual total current, peak vertical electric field, and areal extent are discussed. The currents produced by the TRMM retrieval agree well with the

average individual TS currents presented in Mach et al. (2010) and overall current fractions from land and ocean TSs and ESCs in Mach et al. (2011). Our ability to reproduce the earlier aircraft findings from passive microwave and radar measurements of land-based and oceanic storms suggests a microphysical origin for the variations in storm current generation in these regions. The questions raised in Blakeslee et al. (2014) still remain on why land and ocean storms generate different amounts of current per lightning flash rate.

We estimate that TSs contribute 61% of the total current while ESCs contribute the remaining 39%. Land-based regions account for 38% of the total, and 62% comes from electrified weather offshore. Large MCSs and electrified clouds with individual Wilson currents >1 A and peak electric fields above 1 kVm^{-1} contribute the largest fraction of the total retrieved current. The abundant convective-scale features and weaker electrified clouds in the ECF database are found to have only a minor contribution to the total retrieved current.

The ranking of the tropical chimneys in terms of total retrieved current is (1) the Americas, (2) Asia, and (3) Africa. The remaining Pacific quadrant generates slightly more current than Africa and less than Asia. Africa is ranked first in terms of total lightning, but fourth overall for DC current because it has considerably less ESC activity and because African TSs are slightly smaller and produce weaker retrieved electric fields than their counterparts in the Americas and Asia. The combined effect of a reduced scale and intensity causes average African TSs to generate nearly half the total current as its counterparts in the other two chimneys.

Acknowledgments
This work was partly funded by the National Science Foundation Frontiers in Earth System Dynamics grant AGS-1135446 and NSF grant 1519006. The National Center for Atmospheric Research is sponsored by the National Science Foundation. Data used in this study are hosted at Texas A&M University Corpus Christi and may be accessed at atmos.tamucc.edu/trmm/. We also thank Rich Blakeslee for the valuable insights and guidance provided.

References

Alderman, E. J., & Williams, E. R. (1996). Seasonal variation of the Global Electric Circuit. *Journal of Geophysical Research*, *101*(D23), 29,679–29,688.

Awaka, J., Iguchi, T., & Okamoto, K. (1998). Rain type classification algorithm. *Measuring Precipitation from Space*, *3*, 213–224.

Bailey, J. C., Blakeslee, R. J., Buechler, D. E., & Christian, H. J. (2007). Diurnal lightning distributions as observed by the Optical Transient Detector (OTD) and the Lightning Imaging Sensor (LIS). Paper presented at 13th International Conference on Atmospheric Electricity. Int. Comm. on Atmos. Electr., Beijing.

Baumgaertner, A. J. G., Thayer, J. P., Neely, R. R. III, & Lucas, G. (2013). Toward a comprehensive Global Electric Circuit model: Atmospheric conductivity and its variability in CESM1 (WACCM) model simulations. *Journal of Geophysical Research: Atmospheres*, *118*, 9221–9232. https://doi.org/10.1002/jgrd.50725

Blakeslee, R. J., Driscoll, K. T., Buechler, D. E., Boccippio, D. J., Boeck, W. L., Christian, H. J., et al. (1999). Diurnal lightning distribution as observed by the Optical Transient Detector (OTD), in 11th International Conference on Atmospheric Electricity. NASA Conf. Publ., NASA/CP-1999-209261, 742–745.

Blakeslee, R. J., Mach, D. M., Bateman, M. G., & Bailey, J. C. (2014). Seasonal variations in the lightning diurnal cycle and implications for the Global Electric Circuit. *Atmospheric Research*, *135-136*, 228–243. https://doi.org/10.1016/j.atmosres.2012.09.023

Brooks, C. E. P. (1925). The distribution of thunderstorms over the globe. *Memoirs, Geophysical*, *3*(24), 147–164.

Cecil, D. J., Buechler, D. E., & Blakeslee, R. J. (2014). Gridded lightning climatology from TRMM-LIS and OTD: Dataset description. *Atmospheric Research*, 1350136, 404–414.

Davydenko, S. S., Mareev, E. A., Marchall, T. C., & Stolzenburg, M. (2004). On the calculation of electric fields and currents of mesoscale convective systems. *Journal of Geophysical Research*, *109*, D11103. https://doi.org/10.1029/2003JD003832

Deierling, W., Kalb, C., Mach, D., Liu, C., Peterson, M., & Blakeslee, R. (2014). On the variability of Wilson currents by storm type and phase. 15th International Conference on Atmospheric Electricit, normal, OK. Retrieved from http://www.nssl.noaa.gov/users/mansell/icae2014/preprints/Deierling_77.pdf

Ely, B. L., Orville, R. E., Lawrence, D. C., & Hodapp, C. L. (2008). Evolution of the total lightning structure in a leading-line, trailing-stratiform mesoscale convective system over Houston, Texas. *Journal of Geophysical Research*, *113*, D08114. https://doi.org/10.1029/2007JD008445

Hendon, H., & Woodberry, K. (1993). The diurnal cycle of tropical convection. *Journal of Geophysical Research*, *98*, 16,623–16,637.

Holzworth, R. H., Bering, E. A. III, Kokorowski, M. F., Lay, E. H., Reddell, B., Kadokura, A., et al. (2005). Balloon observations of temporal variation in the global circuit compared to global lightning activity. *Advances in Space Research*, *36*(11), 2223–2228. https://doi.org/10.1016/j.asr.2005.07.009

Hutchins, M. L., Holzworth, R. H., & Brundell, J. B. (2014). Diurnal variation of the Global Electric Circuit from clustered thunderstorms. *Journal of Geophysical Research: Space Physics*, *119*, 620–629. https://doi.org/10.1002/2013JA019593

Israel, H. (1973). Atmospheric electricity, vol. II. Israel program for scientific translations, ltd., 0 7065 1129 8.

Jayaratne, E. R., Saunders, C. P. R., & Hallet, J. (1983). Laboratory studies of the charging of soft hail during ice crystal interactions. *Quarterly Journal of the Royal Meteorological Society*, *109*(461), 609–630. https://doi.org/10.1002/qj.49710946111

Kummerow, C., Barnes, W., Kozu, T., Shiue, J., & Simpson, J. (1998). The Tropical Rainfall Measuring Mission (TRMM) sensor package. *Journal of Atmospheric and Oceanic Technology*, *15*(3), 809–817. https://doi.org/10.1175/1520-0426(1998)015<0809:TTRMMT>2.0.CO;2

Lang, T. J., & Rutledge, S. A. (2008). Kinematic, microphysical, and electrical aspects of an asymmetric bow echo mesoscale convective system observed during STEPS. *Journal of Geophysical Research*, *113*, D08213. https://doi.org/10.1029/2006JD007709

Lang, T. J., Rutledge, S. A., & Wiens, K. C. (2004). Origins of positive cloud-to-ground lightning in the stratiform region of a mesoscale convective system. *Geophysical Research Letters*, *31*, L10105. https://doi.org/10.1029/2004GL019823

Liu, C., Williams, E. R., Zipser, E. J., & Burns, G. (2010). Diurnal variations of global thunderstorms and electrified choswer clouds and their contribution to the Global Electric Circuit. *Journal of the Atmospheric Sciences*, *67*(2), 309–323. https://doi.org/10.1175/2009JAS3248.1

Liu, C., & Zipser, E. J. (2008). Diurnal cycles of precipitation, clouds, and lightning in the tropics from 9 years of TRMM observations. *Geophysical Research Letters*, *35*, L04819. https://doi.org/10.1029/2007GL032437

Liu, C., Zipser, E. J., Cecil, D. J., Nesbitt, S. W., & Sherwood, S. (2008). A cloud and precipitation feature database from 9 years of TRMM observations. *Journal of Applied Meteorology and Climatology*, *47*(10), 2712–2728. https://doi.org/10.1175/2008JAMC1890

Mach, D. M., Blakeslee, R. J., & Bateman, M. G. (2011). Global Electric Circuit implications of combined aircraft storm electric current measurements and satellite-based diurnal lightning statistics. *Journal of Geophysical Research*, *116*, D05201. https://doi.org/10.1029/2010JD014462

Mach, D. M., Blakeslee, R. J., Bateman, M. G., & Bailey, J. C. (2009). Electric fields, conductivity, and estimated currents from aircraft overflights of electrified clouds. *Journal of Geophysical Research*, *114*, D10204. https://doi.org/10.1029/2008JD011495

Mach, D. M., Blakeslee, R. J., Bateman, M. G., & Bailey, J. C. (2010). Comparisons of total currents based on storm location, polarity, and flash rates derived from high-altitude aircraft overflights. *Journal of Geophysical Research*, *115*, D03201. https://doi.org/10.1029/2009JD012240

Mansell, E. R., MacGorman, D. R., Ziegler, C. L., & Straka, J. M. (2005). Charge structure and lightning sensitivity in a simulated multicell thunderstorm. *Journal of Geophysical Research*, *110*, D12101. https://doi.org/10.1029/2004JD005287

Markson, R. (2007). The global circuit intensity: Its measurement and variation over the last 50 years. *Bulletin of the American Meteorological Society*, *88*(2), 223–242. https://doi.org/10.1175/BAMS-88-2-223

Marshall, T. C., Stolzenburg, M., Krehbiel, P. R., Lund, N. R., & Maggio, C. R. (2009). Electrical evolution during the decay stage of New Mexico thunderstorms. *Journal of Geophysical Research*, *114*, D02209. https://doi.org/10.1029/2008JD010637

Mezuman, K., Price, C., & Galanti, E. (2014). On the spatial and temporal distribution of global thunderstorm cells. *Environmental Research Letters*, *9*(12), 124023. https://doi.org/10.1088/1748-9326/9/12/124023

Nesbitt, S. W., & Zipser, E. J. (2003). The diurnal cycle of rainfall and convective intensity according to three years of TRMM measurements. *Journal of Climate*, *16*, 14561475.

Nesbitt, S. W., Zipser, E. J., & Cecil, D. J. (2000). A census of precipitation features in the tropics using TRMM: Radar, ice scattering, and lightning observations. *Journal of Climate*, *13*(23), 4087–4106. https://doi.org/10.1175/1520-0442(2000)013<4087:ACOPFI>2.0.CO;2

Peterson, M., Deierling, W., Liu, C., Mach, D., & Kalb, C. (2017). A TRMM/GPM retrieval of the total mean generator current for the global electric circuit. *Journal of Geophysical Research: Atmospheres*, *122*, 10,025–10,049. https://doi.org/10.1002/2016JD026336

Peterson, M., Deierling, W., Liu, C., Mach, D., & Kalb, C. (2018). Retrieving Global Wilson Currents from Electrified Clouds Using Satellite Passive Microwave Observations. *Journal of Atmospheric and Oceanic Technology*, *35*, 1487–1503. https://doi.org/10.1175/JTECH-D-18-0038.1

Peterson, M., & Liu, C. (2011). Global statistics of lightning in anvil and stratiform regions over the tropics and subtropics observed by the Tropical Rainfall Measuring Mission. *Journal of Geophysical Research*, *116*, D23201. https://doi.org/10.1029/2011JD015908

Peterson, M. J., Liu, C., Mach, D., Deierling, W., & Kalb, C. (2015). A method of estimating electric fields above electrified clouds from passive microwave observations. *Journal of Atmospheric and Oceanic Technology*, *32*(8), 1429–1446. https://doi.org/10.1175/JTECH-D-14-00119.1

Reynolds, S. E., Brook, M., & Gourley, M. F. (1957). Thunderstorm charge separation. *Journal of Meteorology*, *14*(5), 163–178.

Rutledge, S. A., & MacGorman, D. R. (1988). Cloud-to-ground lightning activity in the 10–11 June 1985 mesoscale convective system observed during the Oklahoma-Kansas PRESTORM project. *Monthly Weather Review*, *116*(7), 1393–1408. https://doi.org/10.1175/1520-0493(1988)116<1393:CTGLAI>2.0.CO;2

Saunders, C. P. R., Keith, W. D., & Mitzeva, R. P. (1991). The effect of liquid water content on thunderstorm charging. *Journal of Geophysical Research*, *96*(D6), 11,007–11,017. https://doi.org/10.1029/91JD00970

Saunders, C. P. R., & Peck, S. L. (1998). Laboratory studies of the influence of the rime accretion rate on charge transfer during crystal/graupel collisions. *Journal of Geophysical Research*, *103*(D12), 13,949–13,956. https://doi.org/10.1029/97JD02644

Simpson, G. C. (1929). Discussion on the paper by F.J.W. Whipple, On the association of the diurnal variation of electric potential gradient in fine weather with the distribution of thunderstorms over the globe. *Quarterly Journal of the Royal Meteorological Society*, *55*, 13–15.

Spencer, R. W., Goodman, H. G., & Hood, R. E. (1989). Precipitation retrieval over land and ocean with the SSM/I: Identification and characteristics of the scattering signal. *Journal of Atmospheric and Oceanic Technology*, *6*(2), 254–273. https://doi.org/10.1175/1520-0426(1989)006<0254:PROLAO>2.0.CO;2

Takahashi, T. (1978). Riming electrification as a charge generation mechanism in thunderstorms. *Journal of the Atmospheric Sciences*, *35*(8), 1536–1548. https://doi.org/10.1175/1520-0469(1978)035<1536:REAACG>2.0.CO;2

Takahashi, T., & Miyawaki, K. (2002). Reexamination of riming electrification in a wind tunnel. *Journal of the Atmospheric Sciences*, *59*(5), 1018–1025. https://doi.org/10.1175/1520-0469(2002)059<1018:ROREIA>2.0.CO;2

Whipple, F. J. W. (1929). On the association of the diurnal variation of electric potential gradient in fine weather with the distribution of thunderstorms over the globe. *Quarterly Journal of the Royal Meteorological Society*, *55*, 1–17.

Whipple, F. J. W., & Scrase, F. J. (1936). Point discharge in the electric field of the Earth. *Memoirs, Geophysical*, *68*(7), 1–20.

Williams, E. R. (1998). The positive charge reservoir for sprite-producing lightning. *Journal of Atmospheric and Solar - Terrestrial Physics*, *60*(7-9), 689–692. https://doi.org/10.1016/S1364-6826(98)00030-3

Williams, E. R., & Heckman, S. J. (1993). The local diurnal variation of cloud electrification and the global diurnal variation of negative charge on the Earth. *Journal of Geophysical Research*, *98*(D3), 5221–5234. https://doi.org/10.1029/92JD02642

Williams, E. R., & Satori, G. (2004). Lightning, thermodynamic and hydrological comparison of the two tropical continental chimneys. *Journal of Atmospheric and Solar - Terrestrial Physics*, *66*(13-14), 1213–1231. https://doi.org/10.1016/j.jastp.2004.05.015

Wilson, C. T. R. (1920). Investigation on lightning discharges and on the electric field of thunderstorms. *Philosophical Transactions of the Royal Society A*, *221*, 73–115.

Zipser, E. J., Liu, C., Cecil, D. J., Nesbitt, S. W., & Yorty, D. P. (2006). Where are the most intense thunderstorms on Earth? *Bulletin of the American Meteorological Society*, *87*(8), 1057–1072. https://doi.org/10.1175/BAMS-87-8-1057